Transformation of light paraffins in a microwave-induced plasma-based reactor at reduced pressure

Manuel Mora,[1] María del Carmen García,[2,*] César Jiménez-Sanchidrián,[1] Francisco José Romero-Salguero[1,*]

[1] Department of Organic Chemistry, Faculty of Sciences, University of Córdoba, Campus de Rabanales, Marie Curie Building, Ctra. Nnal. IV, km 396, 14071 Córdoba, Spain

[2] Department of Applied Physics, Polytechnic School, University of Córdoba, Campus de Rabanales, Albert Einstein Building, Ctra. Nnal. IV, km 396, 14071 Córdoba, Spain

* Corresponding authors. Tel.: +34 957212065; fax: +34 957212066. E-mail address: qo2rosaf@uco.es (F. J. Romero-Salguero). Tel.: +34 957212633; fax: 34 957212068. E-mail address: fa1gamam@uco.es (M. C. García).

ABSTRACT

In this work, the effects of the plasma chemistry of an argon microwave (2.45 GHz) discharge at reduced pressure on the conversion of three different alkanes (n-pentane, n-hexane and n-heptane) have been studied. Optical emission spectroscopy has been used for identifying the species generated in the plasma and for estimating its gas temperature. Gas chromatography, mass spectrometry, X-ray diffraction and FTIR spectroscopy have been employed for identifying and analyzing all the compounds present as reaction products. Microwave power and hydrocarbon flow rate have been found critically to affect both conversion and selectivity. The main gas products have been hydrogen and ethylene. At low powers (100-150 W) the conversion to hydrogen has been quite selective. However, at high powers (>300 W) or slow hydrocarbon flow rate ethylene has resulted to be the major product. In most cases, an important fraction of a carbon deposit has been obtained which has been characterized as an amorphous hydrogenated carbon film. Some plausible mechanisms explaining the formation of the main reaction products have been discussed.

Keywords: Surface-wave discharge, microwave plasma, light paraffins, hydrogen, ethylene, amorphous hydrogenated carbon films

1. Introduction

Hydrogen is nowadays widely used in the chemical industry as a raw material (i.e., ammonia synthesis, refining, etc.) and is becoming more and more popular due to its application in fuel cells. Concerning hydrogen production, it should be clearly distinguished between mobile and stationary applications since one of the main drawbacks of hydrogen is its difficult storage. Hydrogen can be produced from hydrocarbons by a variety of processes, such as partial oxidation with air, steam reforming, CO_2 reforming, and pyrolysis [1-4]. Methane is commonly selected as the hydrogen source by steam reforming on nickel catalysts.

Pyrolysis, often also called thermolysis or direct decarbonization, consists in the dissociation of the hydrocarbon to hydrogen and carbon in the absence of an oxidizer (air, water, etc.), thus avoiding the emission of CO and CO_2 [5]. These by-products would impose additional purification steps for hydrogen in order to fulfill some of its end-use applications [6]. In particular, for its application in fuel cell, hydrogen must be of a high purity. Additionally, it would reduce the amount of CO_2 emitted from fossil fuels, so decreasing the needs for its capture or sequestration. Moreover, the carbon produced would be free of sulfur and ash and could be used in a variety of applications or stored in an environmentally safer manner than CO_2. The hydrocarbon decomposition processes can be catalytic or non-catalytic [7,8]. Among the catalysts, nickel is the most common because it provides the highest activity.

In the last years, the use of plasmas in hydrocarbon reforming applications for different purposes (such as growth of carbon nanotubes, deposition of diamond-like carbon films, conversion of methane into more valuable hydrocarbons, or hydrogen production) has northerly increased. Plasma offers an interesting means for producing active species (electrons, ions, free radicals, metastable species or photons) that allows

synthesizing chemicals with high activation energy. Thus, the employ of plasma reactors for the production of H_2 is very attractive, even for on-board applications [9-13]. They have several important advantages, such as their high conversion efficiencies and their possibilities to operate with a broad range of fuels, including higher hydrocarbons [14-18], alcohols [19], ethers [20,21] or biomass [22].

Different types of plasmas have been used for the transformation of hydrocarbons. Glow discharges at atmospheric pressures were successfully used by Nozaki et al. in the growth of carbon nanotubes [23]. Dielectric-barrier discharges have been employed in deposition of amorphous hydrogenated-carbon thin films [24], conversion of methane into more useful chemicals including synthesis gas, gaseous and liquid hydrocarbons and oxygenates [25-28], and in conversion of natural gas to C_2 hydrocarbons [29]. A maximum hydrogen yield of 4 mol of hydrogen per mol of hydrocarbon has been reported in the auto-thermal reforming of isooctane by combining a dielectric barrier discharge on the surface of bimetallic catalysts [16]. Pulsed corona plasmas were used by Zhu et al. [30] to study methane conversion and Sobacchi et al. [31] used them (followed by a catalytic system) for the partial oxidation based reforming of isooctane at atmospheric pressure. Corona discharges have been also resulted to be effective to produce synthesis gas from methane and air together with C_2 hydrocarbons and carbon oxides [32] as well as C_2 hydrocarbons by oxidative coupling of methane [33]. Käning et al. [34] and Ioffe et al. [35] have studied the dissociation of methane in capacitively coupled RF plasmas, and Chiang and Hon have utilized positive direct current (DC) plasmas of methane-hydrogen for diamond deposition [36]. A hydrogen-rich gas can be produced by using a non-thermal gliding arc reactor to convert gasoline under auto-thermal or steam reforming conditions for automotive applications [18]. A periodic pulsed spark discharge has been used for direct conversion of methane

to acetylene or syngas by Kado et al. [37]. Finally, both DC arc and low current plasmatron fuel converters have been used to convert natural gas, gasoline and diesel fuel into a hydrogen-rich gas under partial oxidation conditions [10,11,14]. The application of the plasma catalysis technique, which integrates plasma and thermal catalysis, in hydrocarbon reforming for hydrogen production has been recently reviewed [38].

Microwave induced plasmas (MIPs) have been also employed with similar purposes. Suib and Zerger [39] have study the conversion of methane to higher hydrocarbons by using MIPs. Heintze and Magureanu have investigated the conversion of methane to aromatic hydrocarbons [40] as well as to acetylene [41,42] in a pulsed microwave plasma at atmospheric pressure. Hatano et al. [43] have also claimed the selective conversion of methane to acetylene. Ioffle et al. [44] and Kovács and Deam [45] used MIPs for decomposing methane over carbon. Several authors have employed microwave plasma reactors for hydrogen production by steam reforming [46] or by dry reforming without additives [47,48]. Microwave discharges have been used for the steam reforming of hexane to produce syngas [49]. However, this process requires the subsequent transformation of CO into CO_2 with H_2O with the simultaneous production of H_2 by means of a water-gas shift reaction.

Against other plasmas, in microwave discharges the plasma is not in direct contact with the electrodes which prevents their erosion and the subsequent plasma contamination. Surface Wave Sustained Discharges (SWDs) generated in dielectric tubes are a special kind of MIPs with numerous and interesting features [50]: they can be generated under a broad range of frequency, using different support gases (argon, helium, xenon, nitrogen,…), at different pressure conditions (from few mtorr to several atmospheres), and employing tubes of different shapes (cylindrical or flat) and sizes.

The electromagnetic field that sustains a SWD column is provided by a travelling surface wave linked to the plasma-dielectric interface. This surface wave gradually transmits energy as it propagates throughout the discharge (energy that is partially employed to excite, to ionize and/or to dissociate the different species and molecules existing in the support gas) what provokes a progressively decay of the electron density and temperature (and so of the number of active species) along the plasma column. This feature could be very useful because allows to adapt the design of plasma reactor in order to optimize the results of the application needed, capability that does not have other kind of MIPs, such as those generated at resonant cavities or microwave plasma torches, in which the microwave power is absorbed more uniformly within the whole plasma volume [51].

Often, a surplus of naphtha in the refineries exceeding the needs for its incorporation to the gasoline blend is used for the production of certain hydrocarbons, particularly ethylene, as well as hydrogen. Ethylene is a very useful bulk chemical. It is the organic compound of higher production by virtue of its use as a raw material for the synthesis of very important chemicals, such as polyethylene, ethylene glycol, ethanol or styrene. In fact, more than 70% of the ethylene is currently produced from naphtha. Hydrogen is widely used in refinery for numerous processes (hydrodesulfurization, hydrocracking, hydrogenation, etc.) and is produced in two steps from naphtha, the first one involving its prereforming to hydrogen and methane, and the second consisting in methane to hydrogen conversion via steam reforming. Herein, the transformation of several paraffins in a microwave SWD plasma reactor is reported. In the present work, n-pentane, n-hexane and n-heptane have been chosen as model hydrocarbons of light naphtha. Optical Emission Spectroscopy (OES) techniques have been used in order to gain into the knowledge of the hydrocarbon cleavage process inside the plasma. In the

last years, the employ of optical emission spectroscopy in the plasma process control technology is getting more and more concern. OES is a non-invasive technique (does not affect the plasma) that offers the possibility of observing the plasma in real-time, and whose implementation in the experimental set-up is very simple, since only requires a diagnostic port providing a line-of-sight through the plasma. On the other hand, the combination of OES techniques with GC and mass spectrometry has permitted to get a better understanding of the chemical processes that take place in the post-discharge leading to the production of hydrogen and other hydrocarbons as well as to the deposition of carbon films.

2. Experimental Set-up

2.1. Plasma Reactor design

Figure 1 shows the experimental set-up used for the generation of the plasma. A *surfaguide* device [52] was used to couple the energy coming from a SAIREM GMP 20 KED microwave (2.45 GHz) generator (with a maximun startionary power of 2 kW in continous-wave mode) to the support gas (argon with a purity $\geq$ 99.995 %) within a quartz reactor tube of 12 and 16 mm of inner and outer diameter, respectively. In this work the microwave power ranged from 100 to 500 W levels and a vacuum pump was used to maintain a pressure of about 10 Pa inside the tube. Surface Wave Sustained Discharges of different dimensions were obtained when different amounts of microwave power were injected into the plasma. The movable plunger and stubs permitted the impedance matching so that the best energy coupling could be achieved, making the power reflected back to the generator (P_r) negligible (< 5%). Argon flow rate was set at 100 ml min^{-1}, and was adjusted with a calibrated mass flow controller.

Three different paraffins were introduced into the plasma reactor: n-pentane, n-hexane and n-heptane. The hydrocarbon introduction system consisted in a liquid and a gas mass flow controllers connected to a controlled evaporator mixer (Bronkhorst) and took place at the end part of the plasma column. Argon was used as carrier at 25 ml min^{-1}.

The identification and the analysis of the reaction products were carried out by using a gas chromatograph (Varian 450, equipped with both FID and TCD detectors) and a quadrupole mass spectrometer (OmniStar from Pfeiffer Vacuum) connected on line to the reactor tube. The separation of all compounds was accomplished in a CP-Porabond U capillary column (25 m × 0.32 mm i.d.) with an oven program of 50 to 150 ºC at 4 ºC min^{-1}.

Carbon powders were characterized by X-ray on a Siemens D 5000 diffractometer using Cu Kα radiation as well as by FTIR spectroscopy on a Perkin Elmer FT-IR Spectrum 100 instrument. The hydrogen content was estimated by FTIR applying a multivariate analysis.

The results obtained from the reaction of the paraffins were expressed as follows:

Paraffin conversion = $[F_o(\text{n-paraffin}) - F(\text{n-paraffin})] / F_o(\text{n-paraffin}) \times 100$

where F_o(n-paraffin) and F(n-paraffin), both in mol h^{-1}, denote the flow rates of the paraffin in the feed and the product gas, respectively, and

Production rate = F(product)

where F(product) indicates the flow rate of each compound in the product gas (in mol h^{-1} but g h^{-1} for carbon). Finally, the selectivities to products were defined as follows:

Product selectivity = $F(\text{product}) / [F_o(\text{n-paraffin}) - F(\text{n-paraffin})] \times 100$

2.2. Optical measurements

Light emission from the plasma was analyzed by employing an AvaSpec Multichannel Fiber Optic Spectrometer, configured with three 75 mm focal length spectrometer (Czerny-Turner type) channels, all consisting of 2048 pixel CCD detectors, holographic diffraction gratings of 1200 grooves/mm, and 10 μm slit widths (spectral resolution in 0.1-0.2 nm range). The wavelength ranges for every channel were 300-450 nm, 450-670 nm and 670-850 nm, respectively. Emission from the plasma was side-on collected at different axial position of the plasma column through three optical fibers every one connected to their corresponding spectrometer channel.

Spectra recorded permitted us both to gain knowledge into the different species existing in the plasma and to estimate the plasma gas temperature from the theoretical simulations of CH (4300 Å system) and CN (violet system at 388 nm) spectra and their comparisons to the experimental ones [53,54]. For this purpose, LIFBASE software developed by Luque and Crosley [55] was employed.

3. Results and discussion

3.1. General observations

The introduction of a hydrocarbon (n-pentane, n-hexane, and n-heptane) into the argon SWD had three effects clearly observable: i) the length reduction of the plasma column, ii) the colour change of the light emitted by the plasma and iii) the deposition of carbon films under some experimental conditions.

Theoretically it can be expected that the introduction of molecules (in general) into a pure argon plasma would provoke important changes in its microscopic kinetics because, among others, the energy transfer from electrons to heavy particles (very poor

in argon pure plasmas as a consequence of the big mass difference between electron and argon atoms or ions) could improve due to electron induced vibrational excitation of molecular species. Moreover, the usual ionization/excitation mechanisms of argon atoms will be altered because part of the energy available in the plasma is employed in the processes of dissociation/excitation of molecules.

Upon the introduction of hydrocarbons, the spectra emitted by the plasma were dominated by new molecular bands (what provoked the colour change observed) originated from diatomic species formed inside the plasma. A similar result has been also observed by Timmermans et al. [56] upon introduction of H_2O, N_2 or CO_2 in argon SWDs sustained both at atmopheric and reduced pressures.

3.2. OES analysis

3.2.1. Plasma species

Figure 2 shows the optical emission spectra characteristic of the argon-hexane plasmas studied when microwave powers of 100 and 400 W were injected. They exhibited a relatively strong emission of lines of the Ar I system (corresponding to radiative deexcitation of *4p* and *4p'* levels), of H I system (H_α, H_β and H_γ), and of the molecular bands of NH (3360 Å system, $A^3\Pi \rightarrow X^3\Sigma^-$) and CN (violet system, $B^2\Sigma \rightarrow X^2\Sigma$), and a moderate emission of OH (3060 Å system, $A^2\Sigma^+ - X^2\Pi$), N_2 (second positive system, $C^3\Pi_u \rightarrow B^3\Pi_g$), CH (4300 Å system, $A^2\Delta \rightarrow X^2\Pi$) and C_2 (Swan system, $A^3\Pi_g \rightarrow X'^3\Pi_u$) molecular bands. Atomic carbon lines were not detected in any case. Table 1 summarizes the band heads identified for each molecular band detected and their spectroscopic characteristics. Spectra with similar aspect were detected when experimental conditions were changed (kind of hydrocarbon introduced, microwave power injected or the plasma position considered).

The existence in the spectra of emissions corresponding to species containing nitrogen (N_2, NH, CN) can be understood taking into account that N_2 was present as pollutant at trace level in the argon main gas. The existence of OH impurities inside the plasma was provoked by the plasma-etching of the tube walls.

The presence of N_2 ($C^3\Pi_u$) states in the plasma can be ascribed to excitation transfer from argon metastables (E ~ 11.5 – 11.8 eV) towards ground state of molecular nitrogen (E ~ 11.1 eV) [57-59].

$$Ar^m + N_2 (X^1\Sigma_g^+) \rightarrow Ar^0 + N_2 (C^3\Pi_u) \quad (1)$$

Emissions from N_2 ($C_3\Pi_u$) are enhanced by reaction (1) which results in an enhancement of the emission of N_2 second positive system

$$N_2 (C^3\Pi_u) \rightarrow N_2 (B^3\Pi_g) + h\nu \quad (2)$$

At atmospheric pressure, molecular species NH and CN were likely created by three body association type reactions

$$A + N + S \rightarrow AN^* + S \quad (3)$$

where A (H or C) and N were associated in the presence of a spectator, S.

At reduced pressures, it can be expected the rate of reactions (3) being rather low and inadequate to explain AN molecule formation. Timmermans et al. [56] proposed reactions

$$A + N (+ \text{wall}) \rightarrow AN^* (+ \text{wall}) \quad (4)$$

The formation of NH molecules could be a channel of hydrogen level depopulation.

The green C_2 (Swan) emission proceeded from the radiative decay of $A^3\Pi_g$ level towards ground state $X'^3\Pi_u$

$$C_2 (A^3\Pi_g) \rightarrow C_2 (X'^3\Pi_u) + h\nu \quad (5)$$

The low excitation energy for C_2 ($A^3\Pi_g$) states (2.40 eV) made ground state C_2 could easily be repeatedly excited towards this level likely by electron impact:

$$C_2 (X'^3\Pi_u) + e^- (2.40\ eV) \rightarrow C_2 (A^3\Pi_g) + e^- \quad (6)$$

At reduced pressures, three-body reaction:

$$C + C + X \rightarrow C_2^* + X \quad (7)$$

is inadequate to explain the formation of species C_2 and the strong Swan system detected, because its rate is rather low.

The C_2 ($A^3\Pi_g$) states could be created out of single carbon atoms in a two--particle reaction at the wall quartz tube:

$$C + C\ (+ wall) \rightarrow C_2\ (+ wall) \quad (8)$$

This mechanism has been also proposed by Timmermans et al. [56] for Ar + CO_2 plasmas at low pressure.

Emission of CH (4300 Å system) corresponded to radiative transitions from $A^2\Delta$ levels (3 eV) to the ground state $X^2\Pi$. The presence of methylidyne radical CH inside the plasma can be related to the hydrocarbon dissociation process that was taking place, as will be explained in following sections.

3.2.2. Gas temperatures

By using LIFBASE software, the rotational temperature was determined from theoretical simulations best reproducing profiles of CN and CH experimental spectra. Figure 3 shows the axial evolution of rotational temperatures obtained from CH and CN spectra for the different hydrocarbons injected into the plasma under different experimental conditions of hydrocarbon flow rate. In all the cases studied, the value of rotational temperature measured from CH spectra was of about 1250 K, regardless of the paraffin length or the hydrocarbon flow rate. The values of rotational temperatures obtained from CN spectra were someone higher (around 1400 K), although they showed

the same axial tendency than the previous ones. This small difference is not significant, because it is included within the error range made in the calculations.

In all the cases, rotational temperatures showed a slight tendency to increase with the amount of hydrocarbon injected into the discharge, which is consistent with the thesis that molecule injection improves the energy transfer from electrons to heavy particles.

On the other hand, Figure 4 depicts the rotational temperatures measured from CH and CN rotational spectra when the microwave power injected into the plasma was changed. The values of the gas temperature increased with the microwave power which indicated that the transfer of energy towards heavy particles, inside this plasma in which molecules had been introduced, had improved as predicted previously.

3.3. Transformation of light paraffins

The decomposition of light paraffins, i.e. n-pentane, n-hexane and n-heptane, inside the microwave plasma reactor led to lower hydrocarbons, from C1 to C4, hydrogen and a carbon deposit as a result of pyrolysis reactions. In general, the main hydrocarbon products were methane and particularly a C2 fraction consisting of ethylene and acetylene as well as C3 and C4 hydrocarbons, most of them unsaturated (Figure 5).

The conversion of n-pentane at applied microwave powers from 100 to 450 W is depicted in Figure 6. As can be observed, the conversion increased with the power, being practically constant (ca. 60-65%) above 300 W. At low discharge powers (100-200 W), n-pentane was predominantly transformed into hydrogen and carbon, whereas above 250 W the main product was ethylene (Figure 7). Due to the importance of ethylene in the current petrochemical industry, these results might represent a promising

alternative process to produce it since SWDs are relatively easy to scale-up [51, 60]. In general, the yields to other compounds followed the order: H_2 > acetylene > C_4 > C_3 > methane. Nevertheless, the amount of hydrogen obtained at any power was comparable and in fact at 150 W it could be produced from n-pentane at moderate conversion (ca. 35%) with a high selectivity. Acetylene was not a major product in contrast to the results obtained by other authors in the study of the microwave plasma methane conversion to higher hydrocarbons [39].

Similarly, n-hexane and n-heptane were also transformed in the plasma reactor giving rise to conversions close to 80% at the higher powers (Figure 6). Powers above 200 W produced ethylene as the main reaction product (Figure 7). In these cases, the distribution of products followed the order: H_2 > C_4 > acetylene > C_3 > methane. The amounts of hydrogen obtained were comparable for all hydrocarbons probably because of the analogous H/C ratio of the three paraffins. Prieto et al. [15] obtained hydrogen and ethylene as the major compounds in the non-continuous reforming of heavy oils by using a plate-plate plasma reactor which generated a spark discharge. They found that the selectivity toward both compounds decreased with increasing input power, whereas that to methane and C_{3+} hydrocarbons increased.

At a slower hydrocarbon flow rate, n-hexane was also converted to the same compounds as shown in Figure 7. However, in this case the percentage conversion was usually higher (Figure 6) and the major product was always ethylene.

At low powers, the decomposition of the light paraffins was quite selective towards hydrogen besides the corresponding carbon film deposited on the reactor walls (Figure 8). According to (9), hydrogen could be theoretically obtained in a ca. 16% at the most for the three paraffins. The carbon deposit increased with the power as conversion did (Figure 9). Clearly, at a slower hydrocarbon flow the weight of carbon

generated by decomposition decreased as a result of both the lower mass flow fed to the plasma and the higher ethylene selectivity.

These results could be explained according to the following reaction in the plasma:

$$C_nH_{2n+2} \rightarrow n\,C + (2n+2)\,H \quad (9)$$

if all C-H and C-C bonds were cleaved through collisions with high energy species in the plasma. Afterwards, carbon and hydrogen atoms would recombine in the post-discharge yielding a carbon film and hydrogen. However, it is rather unlikely that the mechanism of full decomposition expressed by reaction (9) would take place because it would not explain the higher selectivity to ethylene at increased microwave powers. On the contrary, the dehydrogenation of the paraffins would better explain the major formation of hydrogen and carbon at low powers:

$$C_nH_{2n+2} \rightarrow H + C_nH_{2n+1} \rightarrow H + C_nH_{2n} \rightarrow \ldots\ C_nH_i\ \ldots \rightarrow H + C_n \quad (10)$$

As power increased, the production of ethylene was greatly enhanced, becoming the main reaction product. Ethylene could be formed by several routes. A carbocationic mechanism by reaction of the hydrocarbon with Ar^+ should be discarded since the product distribution can not be explained by β-scission [61]. Therefore, a free radical mechanism might be proposed. Firstly, it would be expected that the paraffin would crack through collisions with electrons or other excited species in the plasma. Thus, the cleavage of C-C and C-H bonds in the hydrocarbon would result in several radicals:

$$C_nH_{2n+2} \rightarrow a\,C_xH_y\ [x=2 \text{ to } n,\ y=0 \text{ to } (2n+2)] + b\,CH_3 + c\,CH_2 + d\,CH + e\,C + f\,H \quad (11)$$

Hydrogen in the post-discharge seems to come from the coupling of H radicals from the plasma since there is a linear relationship between the intensity of the H_β emission line measured and the H_2 production rate (Figure 10). This is a very interesting result from the point of view of the utility of OES techniques, because the H_2 production in the

reactor could be controlled by means of the emission intensity measurement of the H_β line in the plasma.

C1 species could be subsequently dehydrogenated according to the following equations:

$$CH_3 \rightarrow CH_2 + H \quad (12)$$

$$CH_2 \rightarrow CH + H \quad (13)$$

$$CH \rightarrow C + H \quad (14)$$

and finally by successive reactions, some C_xH_y species would also give CH_z radicals (with z = 0, 1, 2 or 3). However, the formation of methane could be tentatively proposed by hydrogenation of C1 radicals according to:

$$CH_z + (4\text{-}z)\,H \rightarrow CH_4 \quad (15)$$

Although the only C1 radical detected in the plasma by OES was CH, the intensity of the band head of CH (4300 Å system) measured at 431.42 nm correlated quite well with the methane production rate (Figure 10). This relationship has been also found by Chiang et al. [36] and Fantz [62] in plasmas containing methane.

Also, all C2 compounds could be easily formed by coupling of C1 radicals:

$$CH_3 + CH_3 \rightarrow C_2H_6 \quad (16)$$

$$CH_2 + CH_2 \rightarrow C_2H_4 \quad (17)$$

$$CH + CH \rightarrow C_2H_2 \quad (18)$$

However, according to the product distribution, the process described by equation (17), which accounts for the production of ethylene, should prevail. This could be tentatively explained by two reasons: a) the existence of more methylene than methyl groups in all the paraffins studied; and b) the differences in the enthalpies of formation of free radicals and so their stabilities which follow the order: $CH_3 >> CH_2 > CH$ [63]. On the other hand, equation (18) would explain the formation of acetylene. Ethane was absent

in the reaction mixture and so if the process (16) would have taken place, this compound should have been quantitatively dehydrogenated to ethylene, as described by equation (19):

$$C_2H_6 \rightarrow C_2H_4 + H_2 \quad (19)$$

The selective conversion of ethane to ethylene in microwave plasmas has been previously described [39]. Moreover, the dehydrogenation of ethylene to acetylene requires more energy than that of ethane to ethylene. This could explain the high ethylene to acetylene ratio in all hydrocarbon transformations studied in this work.

When comparing the reaction of n-hexane at two different flow rates, it was observed that at a slower hydrocarbon flow rate the selectivity towards ethylene increased whereas that to hydrogen decreased (Figure 8). This fact supports the mechanisms previously proposed because now the same power is applied to a lesser number of molecules, thus favouring reaction (11) more than reaction (10). Also, the acetylene to ethylene ratio was higher for this reaction at low powers, thus indicating a more intense dehydrogenation via reactions (13) and (20):

$$C_2H_4 \rightarrow C_2H_2 + H_2 \quad (20)$$

Higher hydrocarbons, particularly C3 and C4 compounds, could be generated either by coupling of free radicals formed by equations (11)-(14) or by incomplete cleavage of the parent hydrocarbons by scission of only some of their C-C bonds via C_xH_y species generated by equation (11).

The emission of the C_2 (Swan system), species which necessarily comes from the cleavage of C-C and C-H bonds in the parent hydrocarbon, is a good indicator of the extension of the reaction process. The C_2 (Swan system) represents an optical signature of the C-C bond carriers in the plasma [64]. As can be seen in Figure 11, the intensity of C_2 band head at 512.93 nm correlated quite well with the production rates of the carbon-

containing reaction products, i.e. ethylene and carbon deposits. This result agrees with those obtained by Fantz [62] and Chiang and Hon [36], concerning the correlation between the C_2 (Swan system) radiation and C_2 particle densities which are formed by the dissociation of C_2H_y species.

The differences in the reaction mechanisms at lower and higher powers, i.e. the preferential cleavage of C-H or C-C and C-H bonds, respectively, are also supported by the relative emission intensity of the H_β line and C_2 band head at 512.93 nm (Figure 2). Thus, the H_β to C_2 (512.93 nm) intensity ratio was much higher at 100 W (1.9) than at 400 W (0.8).

3.4. Carbon deposits

Just after introducing the feed (n-pentane, n-hexane or n-heptane) in the microwave plasma reactor, a carbon film was deposited on the wall of the quartz tube, although a great part was blown off. XRD patterns of the carbon powders exhibited a low-intensity wide peak centered at ca. $2\theta = 27^\circ$, which can be assigned to the d_{002} difraction of the hexagonal-rhombohedral graphite. No peaks associated to (111), (220) and (311) cubic diamond planes at $2\theta = 43.8°$, 75.4°, and 91.0°, respectively, were seen in the spectrum. Application of the Scherrer equation to the carbon samples obtained from the reactions of n-pentane, n-hexane and n-heptane revealed an average crystallite size of 12, 14 and 18 Å, respectively.

FTIR analysis provided a hydrogen content of ca. 36 at% for the carbon films deposited on the reactor tube, in the range of other carbon films reported previously [65,66]. Deconvolution of the C-H stretching bands in the IR spectra of the carbon powders allowed to estimate the sp^3/sp^2 ratio [67,68]. Thus, the carbon samples comprised about 90% of tetrahedrally coordinated carbon (sp^3), and about 10% of three-

fold coordinated carbon (sp^2). This form of carbon containing a significant fraction of sp^3 bonds and a considerable content in hydrogen is usually named amorphous hydrogenated carbon (a-C:H) and has attracted a great interest due to its mechanical, thermal, and electronic properties, many of which are inbetween those of graphite and diamond [69,70].

4. Conclusions

Surface wave sustained discharges generated in a quartz tubular reactor have been proven to be effective in converting light paraffins, more specifically n-pentane, n-hexane and n-heptane. According to the present study, it can be concluded that:

a) As revealed by OES, when the paraffins are introduced in the argon plasma, the main species generated are H, C_2 and CH radicals besides argon excited atoms (including argon metastables) as well as nitrogen-containing species. Theoretical simulations from CH and CN bands allow to calculate the rotational temperatures which, depending on the microwave power conditions, range from 800 to 1250 K.

b) The overall conversion depends on the applied power and the hydrocarbon flow rate. In some cases, it can be higher than 80%. Regardless of the reacting paraffin, the main products are methane, acetylene and C3 and C4 hydrocarbons but particularly hydrogen and ethylene, both of a great interest for the petrochemical industry. In most cases, a carbon film deposits on the reactor tube.

c) Both microwave power and hydrocarbon flow rate have a marked influence on the selectivity to hydrogen or ethylene. At low powers (100-150 W) the reaction is quite selective towards hydrogen whereas at high powers (>300 W) ethylene can be obtained with selectivities close to 60% at conversions above 70%. A slower flow rate of the

paraffin increases the selectivity to ethylene close to 80%. Interestingly, unlike the results reported by other authors in the transformation of methane, whose coupling leads particularly to acetylene, the most useful ethylene is mainly produced from light paraffins in argon SWDs.

d) Under certain experimental conditions, the transformation of the paraffins produces a carbon deposit which consists of an amorphous hydrogenated carbon film with a high sp^3 coordinated carbon proportion. These materials have potential applications in many areas.

e) OES measurements and product distribution analysis suggest that the mechanism of the reaction proceeds by the cleavage of C-H bonds at low powers and that of C-H and C-C bonds at high powers and the subsequent coupling of the radicals formed. Several factors such as the probability to generate different radicals, their stabilities and the energies involved in all reactions might explain the high selectivity to either hydrogen or ethylene under certain conditions.

Finally, the present study reveals the great perspectives of the SWDs for the transformation of hydrocarbons and for tailoring the selectivity to different products as required. Many other variables can be modified and so these results can be further improved in the near future.

Acknowledgment

The authors wish to acknowledge funding of this research by Ministerio de Ciencia e Innovación (Project MAT2006-04847) and Junta de Andalucía (Project P06-FQM-01741).

REFERENCES

[1] Holladay JD, Hu J, King DL, Wang Y. An Overview of Hydrogen Production Technologies. Cat Today 2009; 139:244-60.

[2] Salazar-Villalpando MD, Reyes B. Hydrogen Production over Ni/ceria-Supported Catalysts by Partial Oxidation of Methane. Int J Hydrogen Energy, 2009; 34: 9723-9729.

[3] Al-Hamamre Z, Voß S, Trimis D. Hydrogen Production by Thermal Partial Oxidation of Hydrocarbon Fuels in Porous Media Based Reformer. Int J Hydrogen Energy, 2009; 34: 827-32.

[4] Roh HS, Lee DK, Koo KY, Jung UH, Yoon WL. Natural Gas Steam Reforming for Hydrogen Production over Metal Monolith Catalyst with Efficient Heat-Transfer. Int J Hydrogen Energy, 2010; 35: 1613-19.

[5] Muradov NZ, Veziroglu TN. "Green" Path from Fossil-Based to Hydrogen Economy: An Overview of Carbon-Neutral Technologies. Int J Hydrogen Energy 2008; 33:6804-39.

[6] Besancon BM, Hasanov V, Imbault-Lastapis R, Benesch R, Barrio M, Molnvik MJ. Hydrogen Quality from Decarbonized Fossil Fuels to Fuel Cells. Int J Hydrogen Energy 2009; 34:2350-60.

[7] Ahmed S, Aitani A, Rahman F, Al-Dawood A, Al-Muhaish F. Decomposition of Hydrocarbons to Hydrogen and Carbon. Appl Catal A: General 2009; 359:1-24.

[8] Abbas HF, Wan Daud WMA. Hydrogen Production by Methane Decomposition: A Review. Int J Hydrogen Energy 2010; in press.

[9] Bromberg L, Cohn DR, Rabinovich A. Plasma Reformer-Fuel Cell System for Decentralized Power Applications. Int J Hydrogen Energy 1997; 22:83-94.

[10] Conh DR, Rabinovich A, Titus CH, Bromberg L. Near-Term Possibilities for Extremely Low Emission Vehicles Using Onboard Plasmatron Generation of Hydrogen. Int J Hydrogen Energy, 1997; 22:715-23.

[11] Bromberg L, Cohn DR, Rabinovich A., Surma JE, Virden J, Compact Plasmatron-Boosted Hydrogen Generation Technology for Vehicular Applications. Int J Hydrogen Energy 1999; 24:341-50.

[12] da Silva CF, Ishikawa T, Santos S, Alves C, Martinelli AE, Production of Hydrogen from Methane Using Pulsed Plasma and Simultaneous Storage in Titanium Sheet. Int J Hydrogen Energy 2006; 31:49-54.

[13] Petitpas G, Rollier J-D, Darmon A, Gonzalez-Aguilar J, Metkemeijer R, Fulcheri L. A Comparative Study of non-Thermal Plasma Assisted Reforming Technologies. Int J Hydrogen Energy 2007; 32:2848-67.

[14] Bromberg L, Cohn DR, Rabinovich A, Heywood J. Emissions Reductions Using Hydrogen from Plasmatron Fuel Converters. Int J Hydrogen Energy 2001; 26:1115-21.

[15] Prieto G, Okumoto M, Shimano K, Takashima K, Katsura S, Mizuno A. Reforming of Heavy Oil Using Nonthermal Plasma. IEEE Trans Ind Applicat 2001; 37:1464-7.

[16] Biniwale RB, Mizuno A, Ichikawa M. Hydrogen Production by Reforming of Iso-octane Using Spray-Pulsed Injection and Effect of Non-Thermal Plasma. Appl Catal A: General 2004; 276:169-77.

[17] Matsui Y, Kawakami S, Takashima K, Katsura S, Mizuno A. Liquid-Phase Fuel Reforming at Room Temperature Using Nonthermal Plasma. Energy Fuels 2005; 19:1561-65.

[18] Paulmier T, Fulcheri L. Use of Non-Thermal Plasma for Hydrocarbon Reforming. Chem. Eng. J. 2005; 106:59-71.

[19] Sarmiento B, Brey JJ, Viera IG, González-Elipe AR, Cotrino J, Rico VJ. Hydrogen Production by Reforming of Hydrocarbons and Alcohols in a Dielectric Barrier Discharge. J Power Sources 2007; 169:140-3.

[20] Song L, Li X, Zheng T. Onboard Hydrogen Production from Partial Oxidation of Dimethyl Ether by Spark Discharge Plasma Reforming. Int J Hydrogen Energy 2008; 33:5060-5.

[21] Zou JJ, Zhang YP, Liu CJ, Hydrogen Production from Partial Oxidation of Dimethyl Ether Using Corona Discharge Plasma. Int J Hydrogen Energy, 2007; 32:958-64.

[22] Van Oost G, Hrabovsky M, Kopecky V, Konrad M, Hlina M. Pyrolysis/Gasification of Biomass for Synthetic Fuel Production Using a Hybrid Gas-water Stabilized Plasma Torch. Vacuum 2009; 83:209-12.

[23] Nozaki T, Kimura Y, Okazaki K. Carbon Nanotubes Deposition in Glow Barrier Discharge Enhanced Catalytic CVD. J Phys D: Appl Phys 2002;35: 2779-84.

[24] Liu DP, Yu SJ, Ma TC, Song ZM, Yang XF. Diamond-like Carbon Films Deposited in the Plasma of Dielectric Barrier Discharge at Atmospheric Pressure. Jpn J Appl Phys Part 1 2000; 39: 3359-60.

[25] Jiang T, Li Y, Liu CJ, Xu GH, Eliasson B, Xue B (2002), Plasma Methane Conversion Using Dielectric-Barrier Discharges with Zeolite. Catal Today, 2002; 72:229-35.

[26] Zou JJ, Zhang YP, Liu CJ. Li Y, Eliasson B. Starch-Enhanced Synthesis of Oxigenates from Methane and Carbon Dioxide using Dielectric- Barrier Discharges. Plasma Chem Plasma Process 2003; 23: 69-82.

[27] Liu C, Eliasson B, Xue B, Li Y, Wang Y. Zeolite-Enhanced Plasma Methane Conversion Directly to Higher Hydrocarbons using Dielectric-Barrier-Discharges. React Kinet Catal Lett 2001; 74:71.

[28] Thayachotpaiboon K, Chavadej S, Caldwell TA, Lobban LL, Mallinson RG. Conversion of Methane to Higher Hydrocarbons in AC Nonequilibrium Plasmas. AIChE 1998; 44: 2252-7.

[29] Wang WB, Xu GH. Conversion of Merthane to C_2 Hydrocarbons via Cold Plasma Reaction. J Natural Gas Chem 2003; 12: 178-82.

[30] Zhu A, Gong W, Zhang X, Zhang B, Coupling of Methane under Pulse Corona Plasma. Science in China (Series B) 2000; 43: 208-14.

[31] Sobacchi MG, Saveliev AV, Fridman AA, Kennedy LA, Ahmed S, Krause T. Experimental Assessment of a Comnined Plasma/Catalytic System for Hydrogen Production via Partial Oxidation of Hydrocarbons Fuels. Int J Hydrogen Energy 2002; 27:635-42.

[32] Supat K, Kruapong A, Chavadej S, Lobban LL, Mallinson RG. Synthesis Gas Production From Partial Oxidation of Methane with Air in AC Electric Gas Discharge. Energy Fuels 2003; 17:474-81.

[33] Liu C, Marafee A, Hill B, Xu G, Mallinson R, Lobban L. Oxidative Coupling of Methane with AC and DC Corona Discharges. Ind Eng Chem Res 1996; 35:3295-301.

[34] Käning M, Röpcke J, Lukas C, Kawetzki T, Shultz-von der Gathen V. Döbele HF, Diagnostic Studies of a Capacitively Coupled RF Plasma containing CH_4-H_2-Ar Part II: On CH_4 Dissociation and Hydrocarbon Plasma Chemistry. Frontiers in Low Temperature Plasma Diagnostics III 1999; Switzerland.

[35] Ioffe MS, Pollington SD, Wan JKS. High-Power Pulsed Radio-Frequency and Microwave Catalytic Processes: Selective Production of Acetylene from the Reaction of Methane over Carbon. J Catal 1995; 151: 349-55.

[36] Chiang MJ, Hon MH. Optical Emission Spectroscopy Study of Positive Direct Current Bias Enhanced Diamond Nucleation. Thin Solid Films 2008; 516: 4765-70.

[37] Kado S, Urasaki K, Sekine Y, Fujimoto K. Direct Conversion of Methane to Acetylene or Syngas at Room Temperature Using Non-equilibrium Pulsed Discharge. Fuel 2003; 82:1377-85.

[38] Chen HL, Lee HM, Chen SH, Chao Y, Chang MB. Review of Plasma Catalysis on Hydrocarbon Reforming for Hydrogen Production—Interaction, Integration, and Prospects. Appl Catal B: Environmental 2008; 85:1-9.

[39] Suib SL, Zerger RP. A Direct, Continous, Low-Power Catalytic Conversion of Methane to Higher Hydrocarbons via Microwave Plasma. J Catal 1993; 139: 383-91.

[40] Heintze M, Magureanu M. Methane Conversion into Aromatics in a Direct Plasma-Catalytic Process. J Catal 2002; 206:91-7.

[41] Heintze M, Magureanu M. Methane Conversion into Acetylene in a Microwave Plasma: Optimization of the Operating Parameters. J Appl Phys 2002; 92:2276-83.

[42] Heintze M, Magureanu M, Kettlitz M. Mechanism of C_2 Hydrocarbon Formation from Methane in a Pulsed Microwave Plasma. J Appl Phys 2002; 92:7022-31.

[43] Onoe K, Fujie A, Yamaguchi T, Hatano Y. Selective Synthesis of Acetylene from Methane by Microwave Plasma Reactions. Fuel 1997; 76:281-2.

[44] Ioffe MS, Pollington SD, Wan JKS. High-Power Pulsed Radio-Frequency and Microwave Catalytic Processes: Selective Production of Acetylene from the Reaction of Methane over Carbon. J Catal 1995; 151: 349-55.

[45] Kovács T, Deam RT. Methane Reformation Using Plasma: an Initial Study. J Phys D: Appl Phys 2006; 39: 2391-2400.

[46] Wang YF, Tsai CH, Chang WY, Kuo YM. Methane Steam Reforming for Producing Hydrogen in Atmospheric-pressure Microwave Plasma Reactor. Int J Hydrogen Energy 2010; 35:135-40.

[47] Jasinski M, Dors M, Mizeraczyk J. Production of Hydrogen via Methane Reforming Using Atmospheric Pressure Microwave Plasma. J Power Sources 2008; 181:41-5.

[48] Tsai CH, Chen KT. Production of Hydrogen and Nano Carbon Powders from Direct Plasmalysis of Methane. Int J Hydrogen Energy 2009; 34:833-38.

[49] Sekiguchi H, Mori Y. Steam Plasma Reforming Using Microwave Discharge. Thin Solid Films 2003; 435:44-8.

[50] Moisan M, Ferreira CM, Hubert J, Margot J, Zakrzewski Z. Surface-Wave Sustained Plasmas: Toward a Better Understanding of RF and Microwave Discharges. XXII Conference on Phenomena In Ionized Gases, Hoboken (N.J.) 1995.

[51] Ferreira CM, Moisan M. Microwave Discharges: Fundamentals and Applications. NATO ASI Series B, Plenum, New York, 1993, Vol. 302.

[52] Fleisch T, Kabouzi Y, Moisan M, Pollak J, Castaños-Martínez E, Nowakowska H; Zakrzewski Z. Designing an Efficient Microwave Plamas Source, Independent of Operating Conditions, at Atmospheric Pressure. Plasma Sources Sci Technol 2007; 16:173-82.

[53] Ricard A. Spectroscopy of Flowing Discharges and Post-Discharges in Reactive Gases. Surf Coat Technol 1993; 59:67-76.

[54] Todorovic-Markovic B, Markovic Z, Mohai I, Karoly Z, Farkas Z, Nikolic Z, Szepvolgyi J. Optical Diagnostic of Fullerene Synthesis in the RF Thermal Plasma Process. J Ser Chem Soc 2005, 70:79-85.

[55] J. Luque and D.R. Crosley, "LIFBASE: Database and Spectral Simulation (version 1.5)", SRI International Report MP 99-009 (1999).

[56] Timmermans EAH, Jonkers J, Rodero A, Quintero MC, Sola A, Gamero A, Schram DC, van der Müllen JAM. The Behaviour of Molecules in Microwave-Induced Plasmas Studied by Optical Emission Spectroscopy 2: Plasmas at Reduced Pressure. Spectrochim Acta B 1999; 54:1085-98.

[57] T.D. Nguyen. Rotational and Vibrational Distributions of N_2 ($C^3\Pi_u$) Excited by State-Selected Ar($^3P_2$) and Ar($^3P_0$) Metastable Atoms. Chem Phys 1983; 79:41-55.

[58] Yu QS, Yasuda HK. An Optical Emission Study on Expanding Low-Temperature Cascade Arc Plasmas. Plasma Chem Plasma Process 1998; 18:461-85.

[59] Kang N, Britun N, Oh S, Gaboriau F, Ricard A. Experimental Study of Ar and Ar-N_2 Afterglow in a Pulse-Modulated ICP Discharge: Observation of Highly Excited Ar(6d) Afterpeak Emission. J Phys D: Appl. Phys 2009; 42:112001(5pp).

[60] Oberreuther T, Wolff C, Behr A. Volumetric Plasma Chemistry with Carbon Dioxide in an Atmospheric Pressure Plasma Using a Technical Scale Reactor. IEEE Trans Plasma Sci 2003; 31:74-8.

[61] Roldán R, Romero FJ, Jiménez-Sanchidrián C, Marinas JM, Gómez JP. Influence of Acidity and Pore Geometry on the Product Distribution in the Hydroisomerization of Light Paraffins on Zeolites. Appl Catal A: General 2005; 288:104-15.

[62] Fantz U. Emision Spectroscopy of Molecular Low Pressure Plasmas. Contrib Plasma Phys 2004; 44:508-15.

[63] CRC Handbook of Chemistry and Physics. 86th ed., Ed. Lide, D. R. CRC Press, Taylor & Francis, Boca Raton, 2005.

[64] Thomas L, Maillé L, Badie JM, Ducarroir M. Microwave Plasma Chemical Deposition of Tetramethylsilane: Correlations between Optical Emission spectroscopy and Film Characteristics. Surf Coat Technol 2001; 142:314-20.

[65] J. Robertson, Properties of Diamond-Like Carbon. Surf Coat Technol 1992; 50: 185-203.

[66] J. Robertson, Deposition Mechanisms for Promoting sp3 Bonding in Diamond-Like Carbon. Diamond and Related Materials 1993; 2:984-989.

[67] Jacob W, Möller W. On the Structure of Thin Hydrocarbon Films. Appl Phys Lett 1993; 63:1771-3.

[68] Lazar G. Influence of the Substrate-electrode Applied Bias Voltage on the Properties of Sputtered a-C:H Thin Films. J Phys: Condens Matter 2001; 13:3011-21.

[69] Robertson J. Diamond-Like Amorphous Carbon. Mater Sci Eng: R 2002; 37:129-281.

[70] Chu PK, Li L. Characterization of Amorphous and Nanocrystalline Carbon Films. Mater Chem Phys 2006; 96:253-77.

Table and figure captions

Table 1. Spectroscopic features of diatomic species observed by OES in the plasma.

Figure 1. Schematic representation of the microwave reactor system.

Figure 2. Optical emission spectra of the argon-hexane plasmas at microwave powers of 100 and 400 W.

Figure 3. Rotational temperatures obtained from theoretical simulations with LIFBASE of CH and CN spectra for the different hydrocarbons fed into the plasma (in position 0) at different flow rates.

Figure 4. Rotational temperatures obtained from theoretical simulations with LIFBASE of CH and CN spectra for n-hexane fed into the plasma ($2.35 \cdot 10^{-2}$ mol h^{-1} in position 0) at different microwave powers.

Figure 5. Typical chromatogram showing the reaction products after introducing n-hexane into the plasma. Both insets depict the analysis of several products by mass spectrometry.

Figure 6. Overall conversion as a function of microwave power for different paraffins and flow rates.

Figure 7. Product distribution as a function of microwave power for different paraffins and flow rates.

Figure 8. Selectivity to different reaction products [left: ethylene; right: hydrogen (solid line) and acetylene (dashed line)] as a function of microwave power for different paraffins and flow rates.

Figure 9. Carbon deposition rates as a function of microwave power for different paraffins and flow rates.

Figure 10. Intensity of the H_β emission line vs. H_2 production rate (black line) and intensity of the CH emission line vs. CH_4 production rate (red line).

Figure 11. Intensity of the C_2 Swan system vs. production rate of ethylene (black line) or carbon (red line).

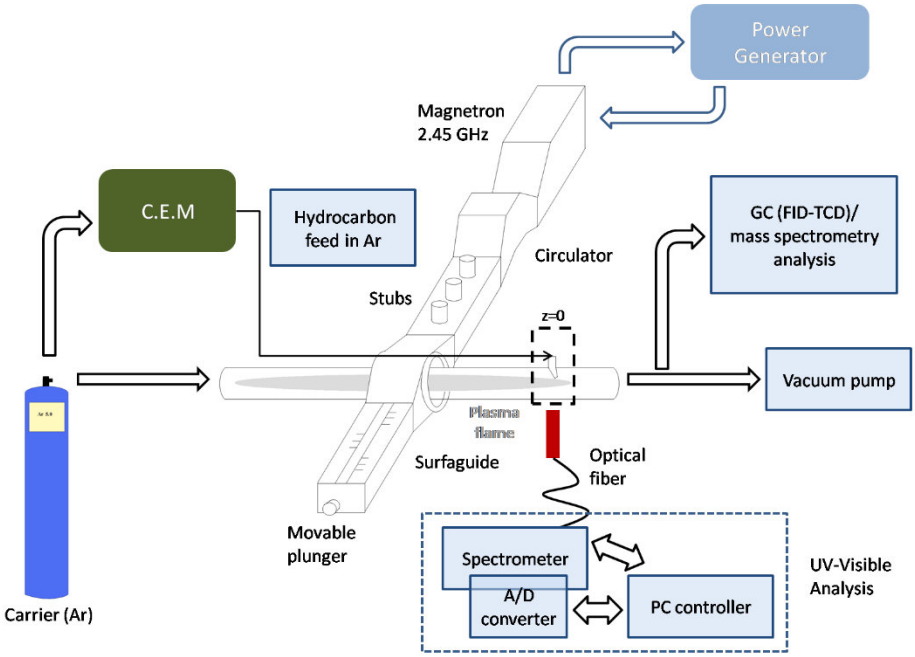
Power Generator
Magnetron 2.45 GHz
C.E.M
Hydrocarbon feed in Ar
Circulator
GC (FID-TCD)/ mass spectrometry analysis
Stubs
z=0
Vacuum pump
Plasma flame
Surfaguide
Optical fiber
Movable plunger
Spectrometer
A/D converter
PC controller
UV-Visible Analysis
Carrier (Ar)

Fig.1

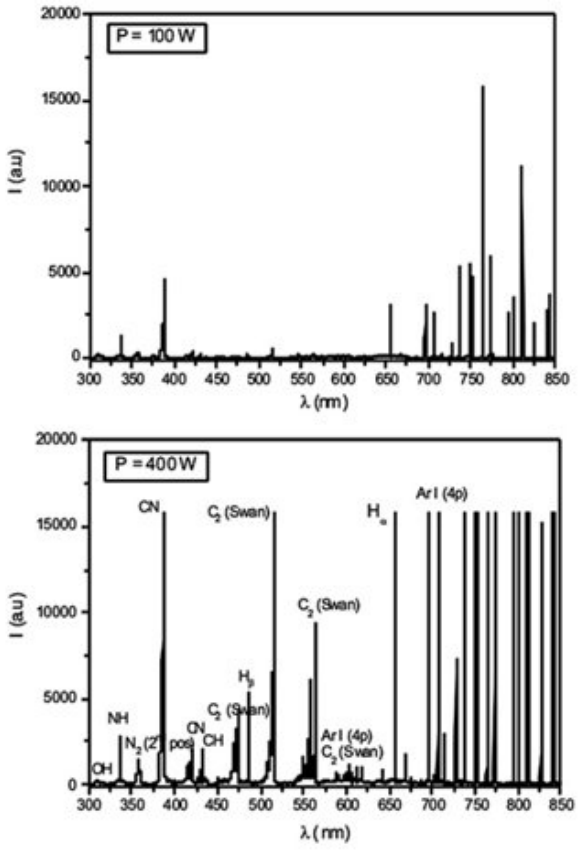
P = 100 W
I (a.u)
λ (nm)
P = 400 W
CN
C2 (Swan)
Hα
ArI (4p)
C2 (Swan)
Hβ
NH
N2 (2+) pos
CN
CH
OH
ArI (4p)
C2 (Swan)

Fig.2

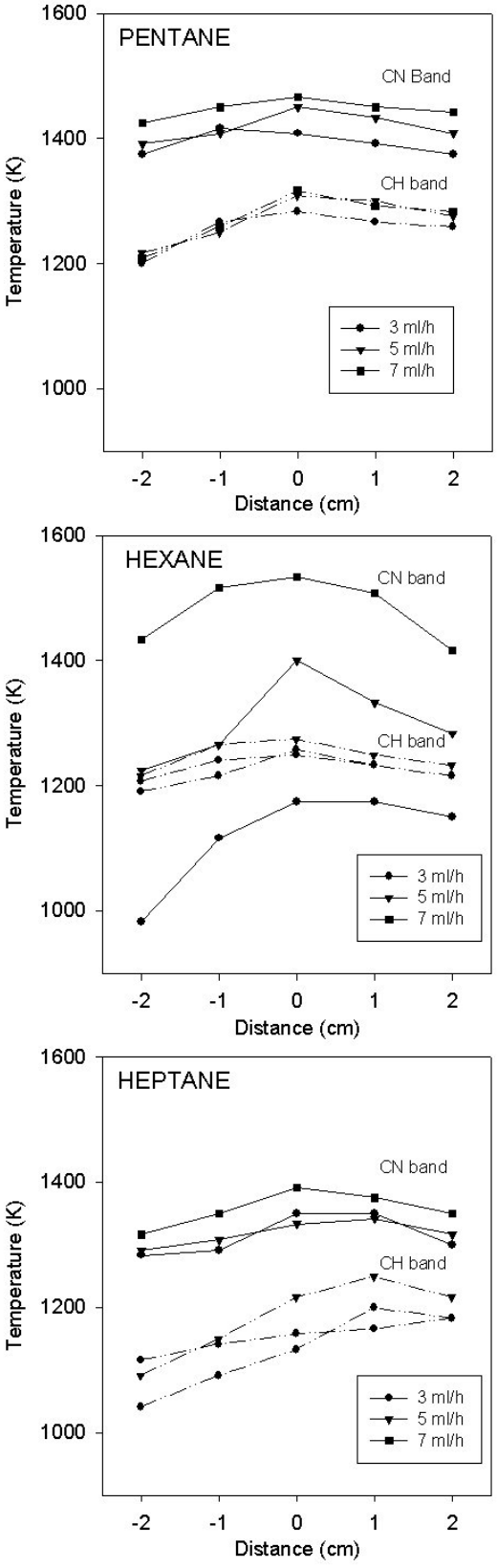
PENTANE
CN Band
CH band
3 ml/h
5 ml/h
7 ml/h
Temperature (K)
Distance (cm)
HEXANE
CN band
CH band
3 ml/h
5 ml/h
7 ml/h
Temperature (K)
Distance (cm)
HEPTANE
CN band
CH band
3 ml/h
5 ml/h
7 ml/h
Temperature (K)
Distance (cm)

Fig.3

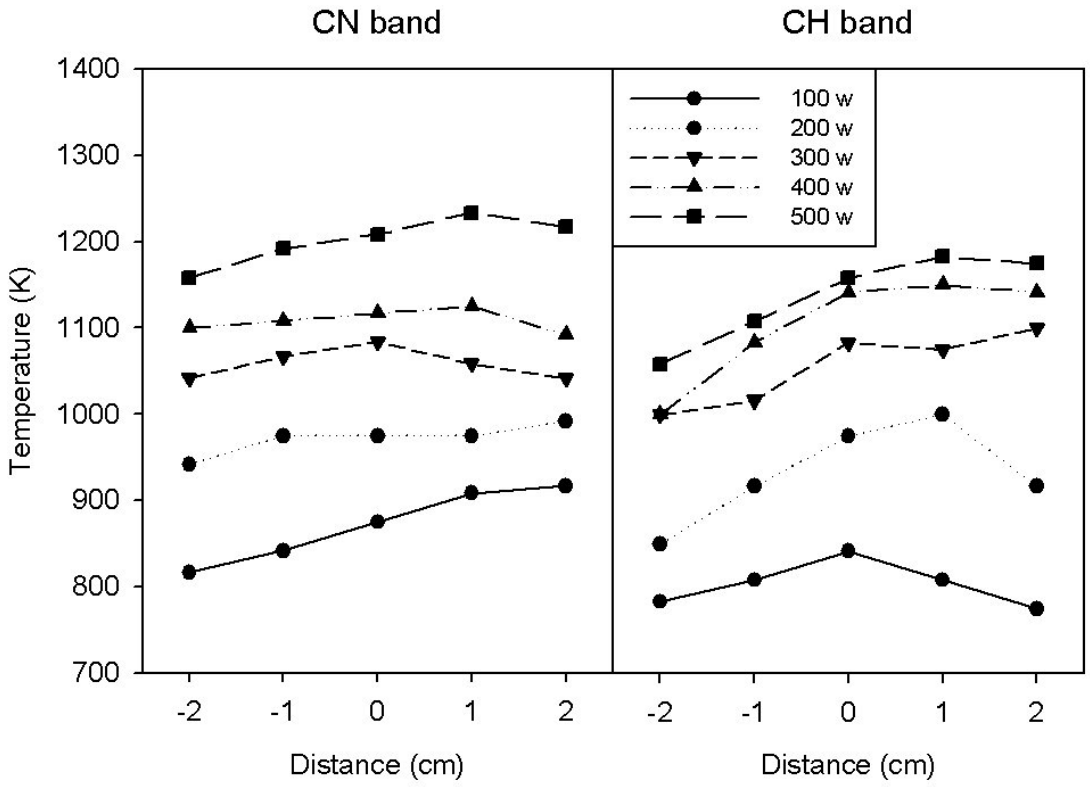
CN band
CH band
100 w
200 w
300 w
400 w
500 w
Temperature (K)
Distance (cm)
Distance (cm)

Fig.4

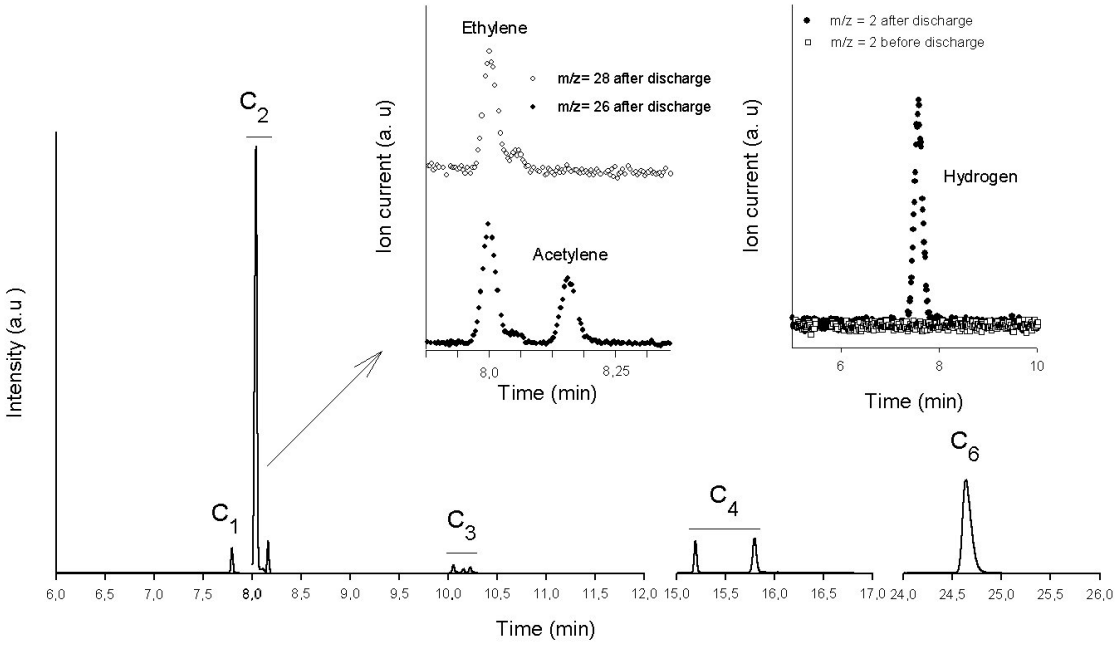
Ethylene
m/z= 28 after discharge
m/z= 26 after discharge
Acetylene
Ion current (a. u)
Time (min)
m/z = 2 after discharge
m/z = 2 before discharge
Hydrogen
Ion current (a. u)
Time (min)
Intensity (a.u)
C1
C2
C3
C4
C6
Time (min)

Fig.5

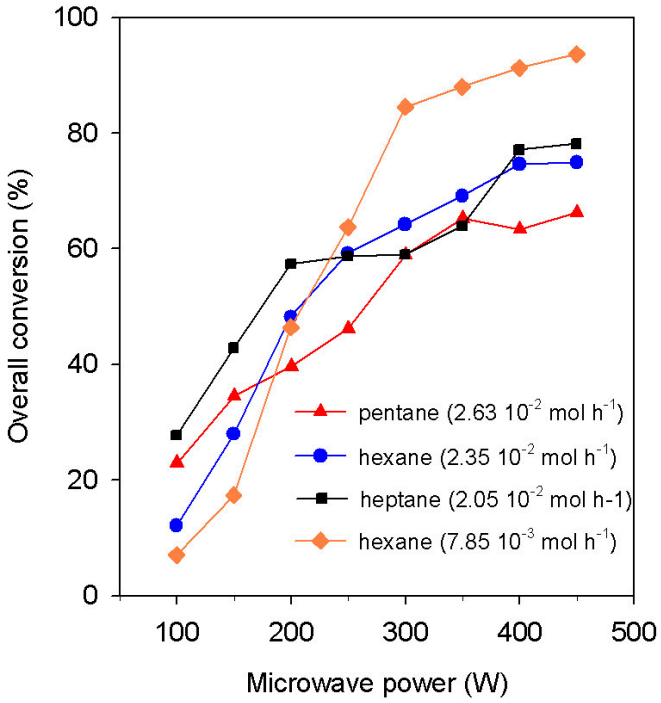
Overall conversion (%)
Microwave power (W)
pentane (2.63 10-2 mol h-1)
hexane (2.35 10-2 mol h-1)
heptane (2.05 10-2 mol h-1)
hexane (7.85 10-3 mol h-1)

Fig.6

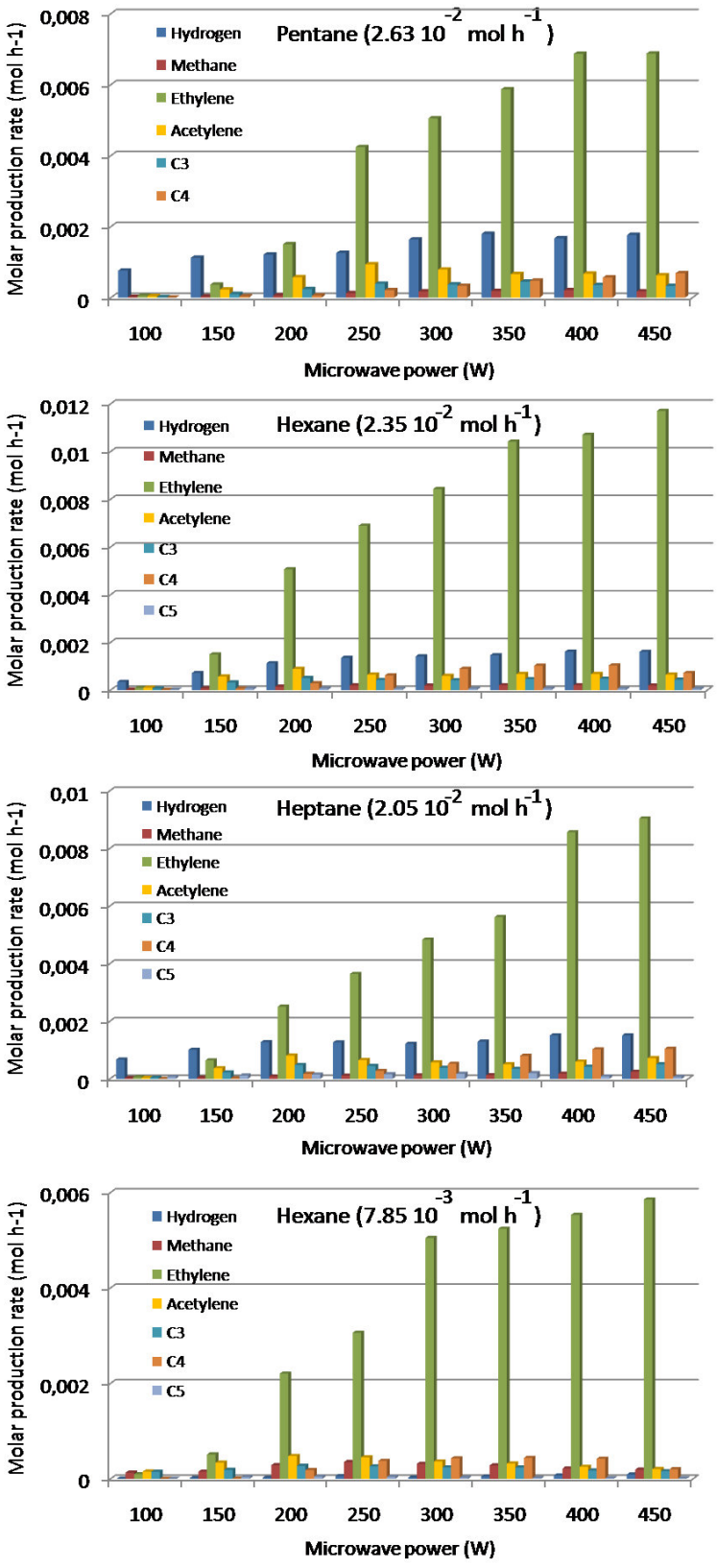
Molar production rate (mol h-1)
0,008
0,006
0,004
0,002
0
Hydrogen
Methane
Ethylene
Acetylene
C3
C4
Pentane (2.63 10-2 mol h-1)
100
150
200
250
300
350
400
450
Microwave power (W)
Molar production rate (mol h-1)
0,012
0,01
0,008
0,006
0,004
0,002
0
Hydrogen
Methane
Ethylene
Acetylene
C3
C4
C5
Hexane (2.35 10-2 mol h-1)
100
150
200
250
300
350
400
450
Microwave power (W)
Molar production rate (mol h-1)
0,01
0,008
0,006
0,004
0,002
0
Hydrogen
Methane
Ethylene
Acetylene
C3
C4
C5
Heptane (2.05 10-2 mol h-1)
100
150
200
250
300
350
400
450
Microwave power (W)
Molar production rate (mol h-1)
0,006
0,004
0,002
0
Hydrogen
Methane
Ethylene
Acetylene
C3
C4
C5
Hexane (7.85 10-3 mol h-1)
100
150
200
250
300
350
400
450
Microwave power (W)

Fig.7

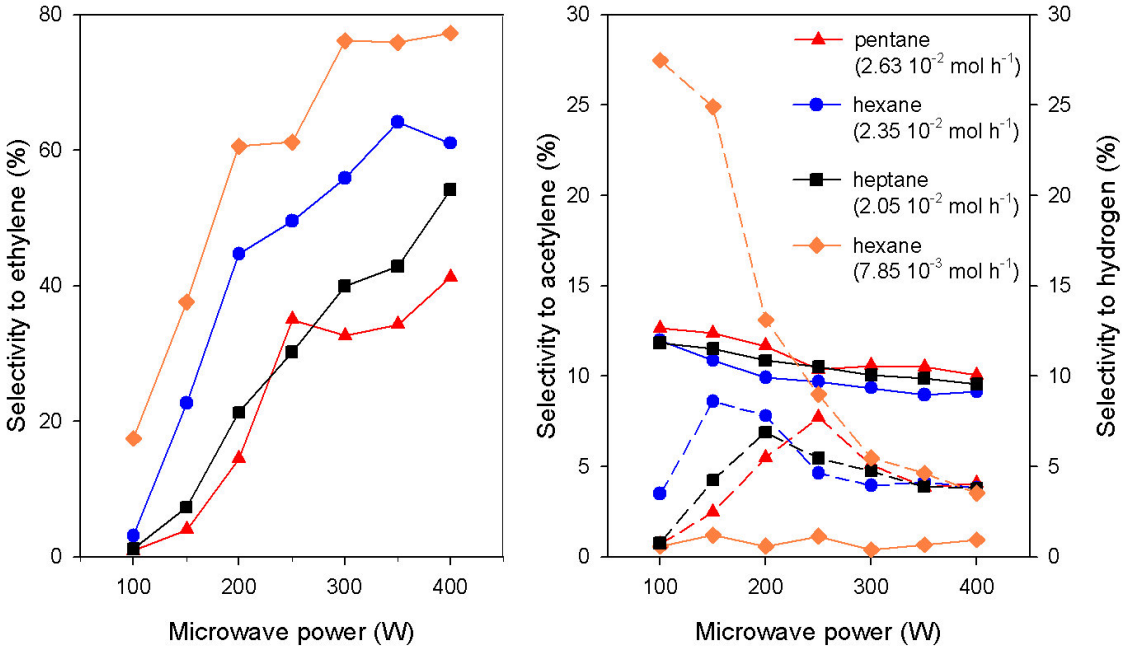
Selectivity to ethylene (%)
Microwave power (W)
Selectivity to acetylene (%)
Selectivity to hydrogen (%)
pentane (2.63 10-2 mol h-1)
hexane (2.35 10-2 mol h-1)
heptane (2.05 10-2 mol h-1)
hexane (7.85 10-3 mol h-1)

Fig.8

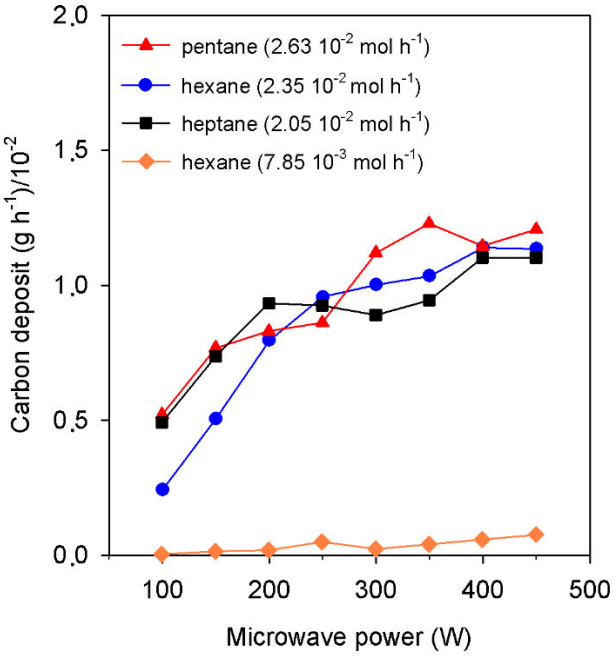
Carbon deposit (g h-1)/10-2
Microwave power (W)
pentane (2.63 10-2 mol h-1)
hexane (2.35 10-2 mol h-1)
heptane (2.05 10-2 mol h-1)
hexane (7.85 10-3 mol h-1)

Fig.9

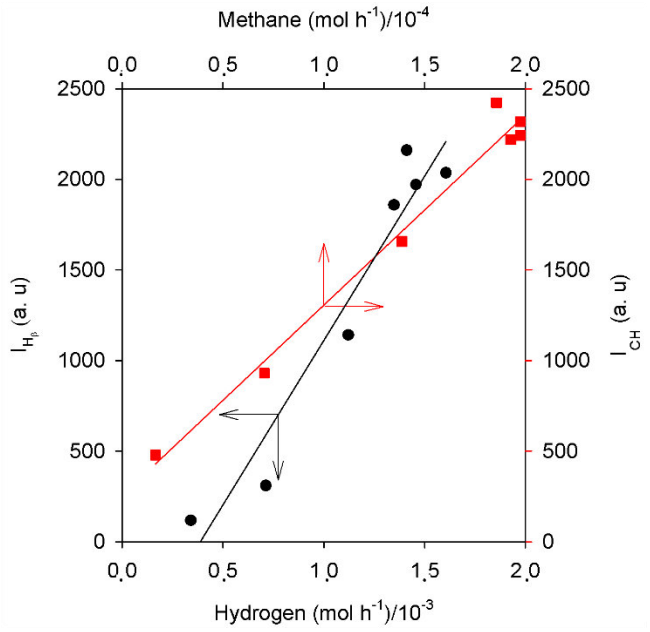
Methane (mol h-1)/10-4
0,0
0,5
1,0
1,5
2,0
2500
2000
1500
1000
500
0
Hydrogen (mol h-1)/10-3
IHβ (a. u)
ICH (a. u)

Fig.10

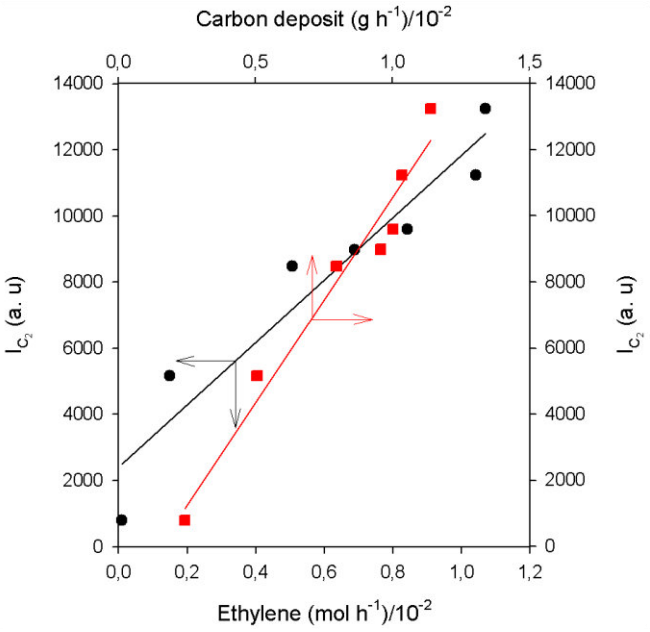
Carbon deposit (g h-1)/10-2
0,0
0,5
1,0
1,5
14000
12000
10000
8000
6000
4000
2000
0
0,2
0,4
0,6
0,8
1,2
Ethylene (mol h-1)/10-2
IC2 (a. u)

Fig.11

Table 1 – Spectroscopic features of diatomic species observed by OES in the plasma.

Species	λ (nm) Band head	Transition	ν', ν''
OH	308.90	$A^2\Sigma^+ \rightarrow X^2\Pi$	0, 0
NH	336.01	$A^3\Pi \rightarrow X^3\Sigma^-$	0, 0
N_2	315.93	$C^3\Pi_u \rightarrow B^3\ \Pi_g$	1, 0
	337.13	$C^3\Pi_u \rightarrow B^3\ \Pi_g$	0, 0
	353.67	$C^3\Pi_u \rightarrow B^3\ \Pi_g$	1, 2
	357.69	$C^3\Pi_u \rightarrow B^3\ \Pi_g$	0, 1
CN	386.19	$B^2\Sigma \rightarrow X^2\Sigma$	2, 2
	387.14	$B^2\Sigma \rightarrow X^2\Sigma$	1, 1
	388.34	$B^2\Sigma \rightarrow X^2\Sigma$	0, 0
	421.60	$B^2\Sigma \rightarrow X^2\Sigma$	0, 1
CH	431.42	$A^2\Delta \rightarrow X^2\Pi$	0, 0
C_2	469.76	$A^3\Pi_g \rightarrow X'^3\Pi_u$	3, 2
	471.52	$A^3\Pi_g \rightarrow X'^3\Pi_u$	2, 1
	473.71	$A^3\Pi_g \rightarrow X'^3\Pi_u$	1, 0
	512.93	$A^3\Pi_g \rightarrow X'^3\Pi_u$	1, 1
	516.52	$A^3\Pi_g \rightarrow X'^3\Pi_u$	0, 0
	550.19	$A^3\Pi_g \rightarrow X'^3\Pi_u$	3, 4
	554.07	$A^3\Pi_g \rightarrow X'^3\Pi_u$	2, 3
	558.55	$A^3\Pi_g \rightarrow X'^3\Pi_u$	1, 2
	563.55	$A^3\Pi_g \rightarrow X'^3\Pi_u$	0, 1
	600.49	$A^3\Pi_g \rightarrow X'^3\Pi_u$	3, 5
	605.97	$A^3\Pi_g \rightarrow X'^3\Pi_u$	2, 4
	612.21	$A^3\Pi_g \rightarrow X'^3\Pi_u$	1, 3
	619.12	$A^3\Pi_g \rightarrow X'^3\Pi_u$	0, 2

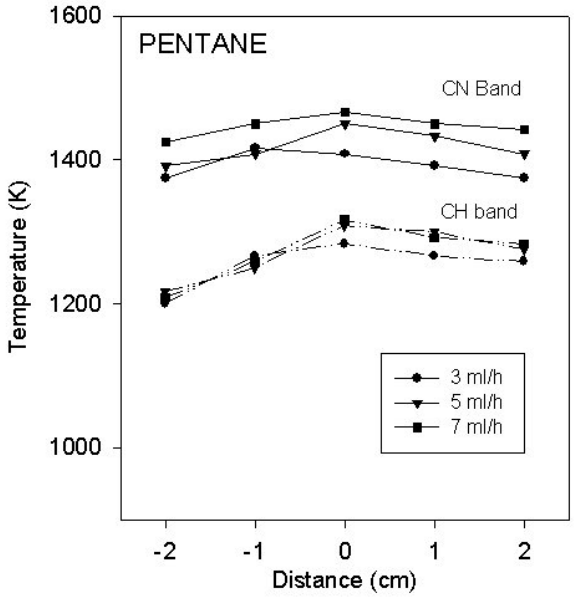
PENTANE
CN Band
CH band
3 ml/h
5 ml/h
7 ml/h
Temperature (K)
Distance (cm)
1600
1400
1200
1000
-2
-1
0
1
2

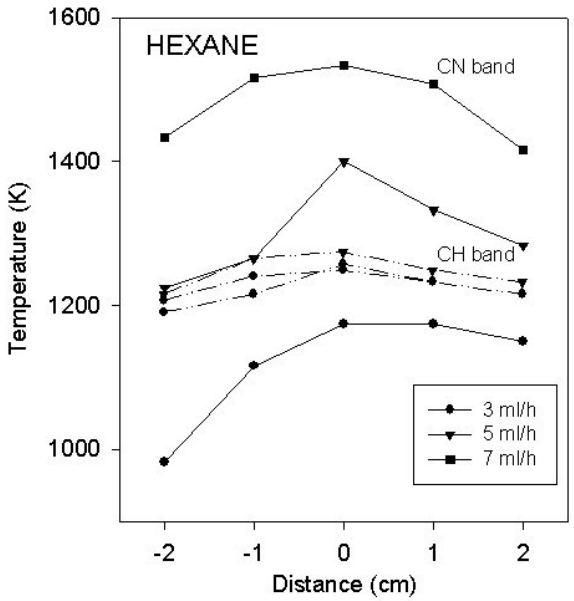
HEXANE
CN band
CH band
3 ml/h
5 ml/h
7 ml/h
Temperature (K)
Distance (cm)
1600
1400
1200
1000
-2
-1
0
1
2

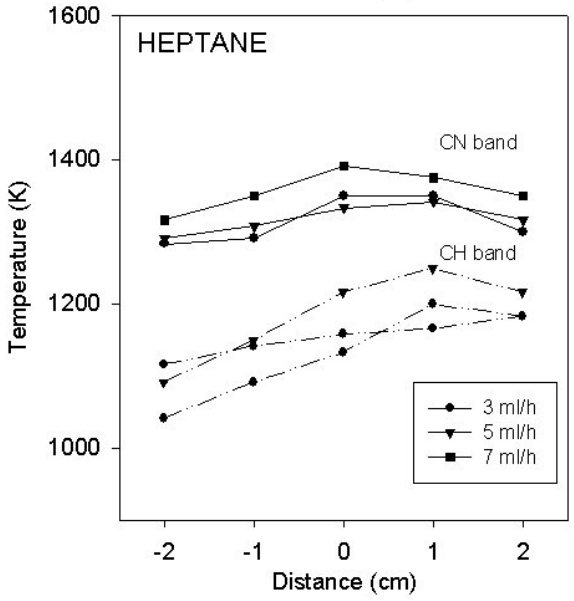
HEPTANE
CN band
CH band
3 ml/h
5 ml/h
7 ml/h
Temperature (K)
Distance (cm)
1600
1400
1200
1000
-2
-1
0
1
2